

## Voltage-Clamp Experiments in Denervated Frog Tonic Muscle Fibres

J. ZACHAR<sup>1</sup>, D. ZACHAROVÁ<sup>1</sup>, M. HENČEK<sup>1</sup>, G. A. NASLEDOV<sup>2</sup> and M. HLADKÝ<sup>3</sup>

<sup>1</sup> Institute of Normal and Pathological Physiology, Centre of Physiological Sciences, Slovak Academy of Sciences, Sienkiewiczova 1, 813 71 Bratislava, Czechoslovakia

<sup>2</sup> Sechenov Institute of Evolutionary Physiology and Biochemistry, Academy of Sciences of the USSR, Thorez pr. 44, 194 223 Leningrad, USSR

<sup>3</sup> Biomathematical Laboratory, Centre of Physiological Sciences, Slovak Academy of Sciences, Vlárská 3, 833 06 Bratislava, Czechoslovakia

**Abstract.** Membrane currents in denervated slow (tonic) muscle fibres from the m. ileofibularis of the frog (*Rana temporaria*) were recorded and analysed by means of the vaseline-gap voltage clamp method. It was confirmed, that in normal fibres the inward current is absent. The potassium conductance-voltage relation,  $G_K-V$ , in cut muscle fibre segments is characterized by the following parameters: e-fold for 10 mV,  $V_{0.5} = -15$  mV and maximum  $G_K$ ,  $\bar{G}_K$  about 0.2 mS/cm<sup>2</sup> at 16°C. The inward currents which appear after denervation (15 days) can be abolished by tetrodotoxin (30 μmol/l). The reversal potential was  $78 \pm 7$  mV. Sodium conductances ( $G_{Na}$ ) as functions of both time and voltage were found to be described quantitatively by the Hodgkin-Huxley model for the sodium channel, i.e. according to the equation  $G_{Na} = \bar{G}_{Na} m^3 h$ , where  $m$  and  $h$  obey first order differential equations.  $\bar{G}_{Na}$  has a value about 10 mS/cm<sup>2</sup>. Parameters of the kinetic model in slow fibres differ from those in twitch fibres by values of the rate constants, what explains slower activation and inactivation of new sodium channels in denervated slow fibres. Results of the kinetic analysis support the hypothesis that the new sodium channels are of the same genetic origin as the sodium channels present under physiological conditions.

**Key words:** Slow (tonic) muscle fibre — Denervation — Sodium channel — Voltage clamp — Hodgkin-Huxley model

### Introduction

Slow (tonic) fibres of the frog are not able to generate action potentials as first observed by Kuffler and Vaughan Williams (1953) and confirmed afterwards by several authors (see reviews by Zhukov 1969; Hess 1970; Zachar 1971; Costantin 1975; Lännergren 1975; Nasledov 1981). The ionic currents registered under voltage clamp conditions which underly the active membrane response are due to

the activation of fast and slow components of the potassium conductance (Gilly and Hui 1980). The action potentials appear, however, after denervation (Miledi et al. 1971; Schmidt and Tong 1973; Nasledov and Thesleff 1974) and are blocked by tetrodotoxin (Schalow and Schmidt 1975). After reinnervation, the sodium action potentials disappear (Schmidt and Stefani 1976; 1977). The action potentials, however, fail to appear when the animals were injected during denervation with actinomycin D (Schmidt and Tong 1973; Nasledov and Thesleff 1974), which is known to block the transcription of genetic information from DNA to RNA (Reich et al. 1967; Thesleff 1974). Synthesis of the sodium channel proteins in innervated tonic fibres appears therefore suppressed by the action of the innervating nerve cells (Schmidt and Tong 1973). When this inhibitory effect is released by denervation the genetic information is expressed and new sodium channels are formed. The proposed hypothesis could be tested by comparing the properties of sodium channels which appear after denervation in tonic (slow) fibres with those expressed physiologically in other excitable membranes of the same animal.

The aim of the experiments reported in this and the subsequent papers (Zacharová et al. 1983; Henček et al. 1983) was therefore to characterise the sodium channels in the muscle membrane of slow (tonic) frog fibres after denervation under voltage clamp conditions. This paper describes the kinetics and the following one the selectivity of new sodium channels which appear after denervation.

## Material and Methods

### *Dissection*

Experiments were performed on single muscle fibres isolated from the tonic bundle of the m. ileofibularis of the frog (*R. temporaria*) as described elsewhere (Nasledov et al. 1966). After the number of fibres in the tonic bundle was reduced to 20–30, the slow fibres were identified by maintained contracture in high potassium saline (80 mmol/l). The phasic fibres which relaxed after a transient contracture under these conditions were cut and after reintroduction of normal saline separated from the tonic fibres. To identify tonic fibres high potassium saline was introduced mostly once for a few minutes only.

### *Denervation*

The tonic fibres in the m. ileofibularis were denervated either by cutting away a short segment from the n. ischiadicus or from the nerve branch to the m. ileofibularis. The surgery was performed under ether anaesthesia. The denervated muscle was excised for dissection after 14 days, when all tonic fibres are known to generate action potentials (Nasledov and Thesleff 1974).

### *Experimental arrangement*

After the dissection was completed the isolated fibre was kept for 30–60 minutes in Ca free saline. The



which allow the temperature of the fibre to be changed rapidly (it takes few tenth seconds only to change the temperature to 10°C) and to maintain the chosen temperature with a high accuracy. These parameters were achieved by construction of the chamber. A perspex plate was glued onto a copper plate; grooves were then fraised in the perspex so that the perspex bottom was about 150–200 µm thick. The small thickness ensures better thermic conductivity between the Peltier elements and the fibre bath.

### *Voltage clamp*

The electrical part of the set-up comprised several operational amplifiers and compensating circuits in principle similar to that described earlier (Henček and Zachar 1977). The operational amplifier A1 with variable frequency characteristics (Gulíšek and Henček 1973) keeps point D (inside of the fibre) at virtual ground. Operational amplifier A2 is of similar construction, and is used to mix required voltages at the electrode *V* (from stimulators and holding potential source). A3 is a symmetrical operational amplifier which measures the ionic current *I*, as voltage drop across the 10 kohm resistor. The ionic current can be also measured at point *I'* as voltage drop across the resistance  $R_{DE}$ . This resistance cannot be measured directly, it can be only estimated from the measured resistance  $R_{EC}$  and the fibre-chamber geometrical data.

The voltage sources  $U_1$ ,  $U_2$ ,  $U_3$  serve to obtain currentless state of the entire system by compensating electrode potentials. They were constructed as 'floating batteries' using semi-conductor circuits fed from a common  $\pm 15$  V DC-source. Switches  $S_0$ – $S_2$  disconnect electrodes from the system during DC compensation. Compensation is performed as follows. Switches  $S_1$  and  $S_2$  are off,  $S_0$  connects the input of the amplifier A1 with ground. The feedback potentiometer slider (*F*) is in the bottom position (ground). The amplifier A1 is then compensated by the "zero" potentiometer so as to obtain zero deviation on the constantly connected measuring device (*M*). After switching  $S_0$  on, the amplifier output indicates the summed electrode potentials in the compartments C and B. The deviation is compensated by means of  $U_3$ . The current electrode is then connected through switch  $S_1$  and its potential is compensated by counter current from  $U_1$ . The same operation is then performed with the potential electrode (switch  $S_2$  and source  $U_2$ ). Only if the measuring device indicates zero deviation after this procedure with all the electrodes connected, the adjustment can be "preserved" by turning the feedback potentiometer *F* to upper position. Care must be taken not to let the amplifier A1 to oscillate, while installing the amplification to the broadest frequency band possible. When working with intact fibres, this step brings the system to the voltage clamp regime, and ionic currents can be measured. When working with cut fibres, the potential of the voltage electrode should be shifted to the required holding potential  $V_h$ , using the DC source of  $V_h$ , and after the steady state is reached, the ionic currents can be measured as well.

The ionic currents and the clamping voltages were recorded on the storage oscilloscope screen in parallel with the A/D converter and the computer.

### *Solutions*

The solutions are referred to as external solution // internal solution. The Ringer solution had the following composition (in mmol/l):  $Na^+$  120,  $K^+$  2.5;  $Ca^{2+}$  1.8;  $Cl^-$  121; TRIS<sup>+</sup> 4; pH 7.1. The external K free solution which was mostly used in cut muscle fibre segments contained (in mmol/l): NaCl 110;  $CaCl_2$  2; CsCl 4; TRIS 4; pH = 7.2 (referred to as solution A). The 'internal' solution had the following composition (in mmol/l): Cs glutamate 108;  $MgCl_2$  6.5;  $CaCl_2$  0.069; EGTA 0.2; ATP 5; glucose 5; PIPES 20; TRIS to obtain pH = 7.1–7.2. This solution is referred to as solution D. The use of differently composed solutions is indicated in the text. Tetrodotoxin (TTX) was used in concentration 30 µmol/l.

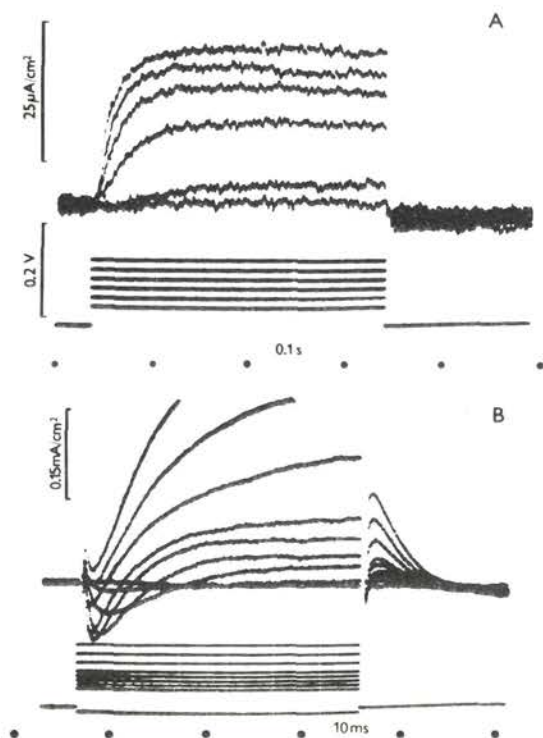
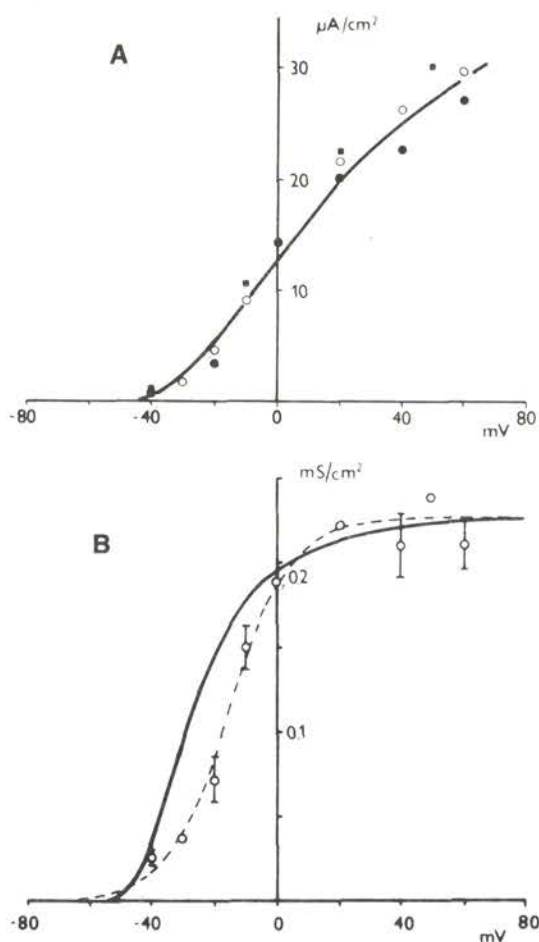


**Fig. 2.** Records of membrane currents under voltage clamp conditions in cut muscle fibre segments. *Upper records:* superimposed membrane currents; *lower records:* voltage clamp pulses. A — slow (tonic) muscle fibre before denervation. B — slow (tonic) muscle fibre 15 days after denervation. Holding potential  $-80$  mV (both in A and B).  $t = 16^{\circ}\text{C}$ .

## Results

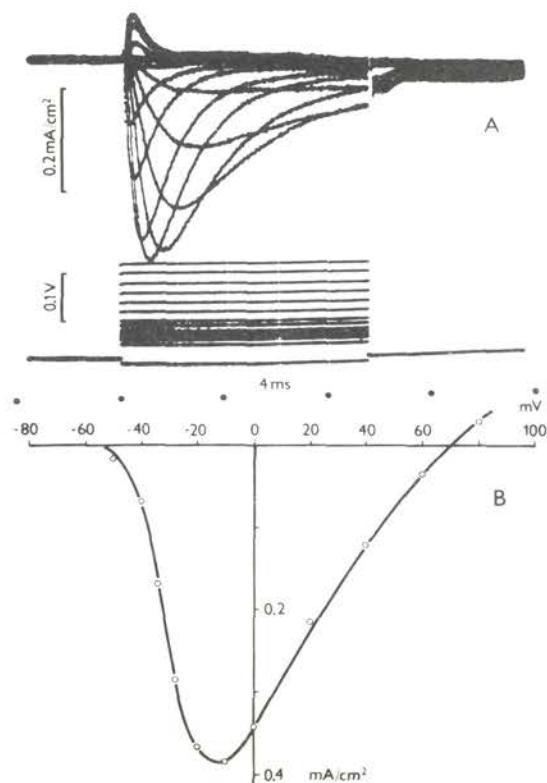
### *Membrane currents in normal tonic fibres*

Fig. 2A shows a series of membrane currents recorded under voltage-clamp conditions at six different clamping voltages in cut muscle fibre segments. Only the outward current is activated, the inward current being absent. With the present method the separation of the linear capacitive currents from the early ionic currents is relatively easy; nevertheless we did not obtain evidence of inward ionic currents of any sort in slow fibres. The outward current of tonic fibres reaches smoothly a steady amplitude during the pulse. With pulses lasting less than 1 s the inactivation of the outward current is very small. The records thus resemble those registered in intact tonic fibres with the three-electrodes voltage clamp method



**Fig. 3.** Membrane current-voltage relation (*a*) and conductance-voltage,  $G_K$ - $V$ , relation (*b*) in slow fibres of the frog. Cut muscle fibre segments. *a*: The full line was drawn by eye. Different symbols denote different fibres. *b*: The continuous curve was calculated using the equation (1) from the data of Adrian et al. (1970). The interrupted line is the best fit line through the mean values ( $\pm$  SEM).

(Gilly and Hui 1980) except for the hump on the rising phase of the outward current. Membrane current-voltage relation from final currents is shown in Fig. 3A. The reversal potential ( $V_K$ ) of the  $\text{K}^+$  current is close to the value of  $-75$  mV found by Gilly and Hui (1980). The chord conductance  $G_K$  calculated by means of this value from the ionic currents follows a sigmoid curve (Fig. 3B) with maximal steepness 10 mV per e-fold change,  $V_{0.5} = -15$  mV and the saturating value of  $G_K$ ,  $\bar{G}_K = 0.23$   $\text{mS}/\text{cm}^2$  at  $16^\circ\text{C}$ . Gilly and Hui (1980) found a lower



**Fig. 4.** Superimposed inward currents in denervated slow muscle fibre membrane (A) and corresponding membrane current-voltage relation (B). Cut muscle fibre segment equilibrated with solution A // K free internal saline. 15 days after denervation.  $t = 16^\circ\text{C}$ .

steepness, 15 mV per e-fold change,  $V_{0.5}$  about +10 mV and higher  $\bar{G}_K = 0.7 \text{ mS/cm}^2$  at  $9.6^\circ\text{C}$  in intact slow fibres in comparison with our results on cut muscle fibre segments. The steepness of the  $G_K - V$  relation (interrupted line in Fig. 3B) is close to the value found in twitch muscle fibres as demonstrated by the full line calculated from the data of Adrian et al. (1970) for  $16^\circ\text{C}$  by means of the equation

$$G_K/\bar{G}_K = n^4 = [\alpha_n/(\alpha_n + \beta_n)]^4, \quad (1)$$

where  $\alpha_n$  and  $\beta_n$  are the transfer rate constants, and  $\bar{G}_K$  is the maximum value of  $G_K$  determined by the best fit curve calculated by  $G_K = \bar{G}_K / \{1 + \exp[(V - V_K)/k]\}$ . The continuous curve is shifted by about 15 mV to more negative potentials. The value of  $\bar{G}_K$  is an order of magnitude lower than in twitch fibres and makes up about 1/3 of the mean value reported by Gilly and Hui (1980) for intact fibres.

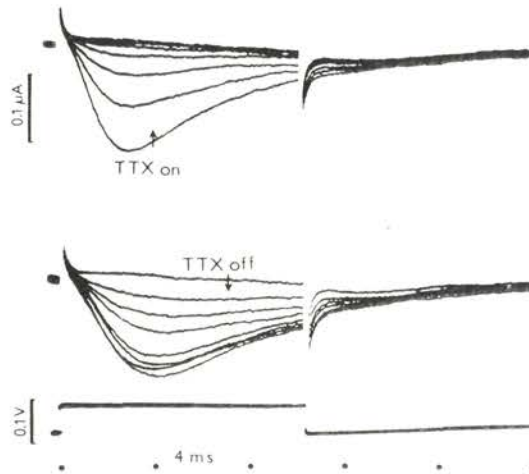


**Fig. 5.** The effect of tetrodotoxin (TTX) on inward currents in denervated slow fibres of the frog ( $10^{-7}$  g/ml). Membrane currents were recorded in 1 s intervals after application of TTX solution or withdrawal of TTX from the solution bathing the testing membrane area.  $t = 16^{\circ}\text{C}$ .

#### *Membrane currents in denervated tonic fibres*

Fig. 2B shows a series of total membrane currents in a slow muscle fibre membrane 15 days after denervation. The most conspicuous change concerns the appearance of inward current, which precedes the outward current component. The outward currents disappear in  $\text{K}^+$  free external and internal medium as demonstrated in Fig. 4A. The currents which remain are sodium currents as evidenced by the effect of TTX. The inward currents are completely abolished by  $10^{-7}$  g/ml TTX (Fig. 5; above). The TTX block is reversible (Fig. 5; below) with the time constant of the 'off' effect comparable to that of the 'on' effect. The successive sweeps in Fig. 5 were registered in 1 s intervals.

The membrane current voltage relation of the peak sodium currents is given in Fig. 4B. In this particular case the reversal potential was +72 mV. The average equilibrium potential was  $78 \pm 7$  mV ( $n = 15$ ).

The sodium inward currents in denervated tonic muscle fibres resemble those in phasic muscle fibres. The rate of rise and decay of  $I_{\text{Na}}$  in slow fibres is, however, about an order of magnitude slower in comparison with twitch fibres. The kinetic parameters thus represent an important identification mark of tonic fibres after denervation. The other features of tonic fibres which make the differentiation between tonic and phasic fibres possible are: the low  $I_{\text{Na}}$  amplitude and the long lasting potassium contracture showing, however, incomplete relaxation (Lapshina and Nasledov 1978). The kinetics of  $I_{\text{Na}}$  in phasic fibres after denervation (Henček

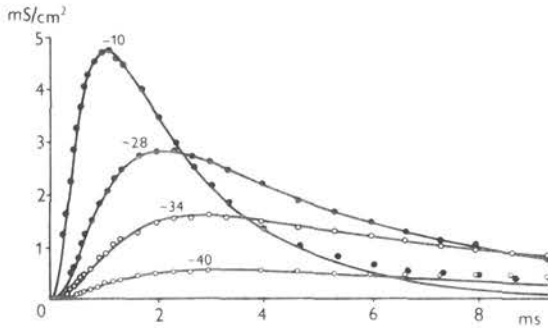


**Fig. 6.** Sodium conductances as functions of time at different depolarizations. Circles represent experimental values. The full lines are theoretical curves (equation 10) with parameters shown in Table 1. The numbers on the curves denote membrane potentials in mV.

et al. 1983) excludes the possibility that the inward currents attributed to slow fibres were recorded from phasic fibres.

#### *Voltage dependence of sodium conductance*

The dependence of sodium channel conductance,  $G_{Na}$ , on the membrane potential is demonstrated in Fig. 6. Circles are experimental values obtained by means of the equation

$$G_{Na} = I_{Na} / (V - V_{Na}), \quad (2)$$

where  $V$  is the membrane potential and  $V_{Na}$  is the reversal potential of the sodium current. The full lines are the best fit lines according to the Hodgkin-Huxley mathematical model

$$G_{Na} = \bar{G}_{Na} m^3 h, \quad (3)$$

where  $\bar{G}_{Na}$  is the maximum sodium conductance expected if all the channels were open;  $m$  and  $h$  are variables which obey a first order differential equation

$$\frac{dm}{dt} = \alpha_m(1 - m) - \beta_m(m), \quad (4)$$

$$\frac{dh}{dt} = \alpha_h(1 - h) - \beta_h(h), \quad (5)$$

**Table 1.** Analysis of sodium conductance curves

Curve	V (mV)	$G'_{Na}$ (mS/cm <sup>2</sup> )	$m_{\infty}$	$\tau_m$ (ms)	$\tau_h$ (ms)
<i>a</i>	-40	0.9	0.446	0.95	8.5
<i>b</i>	-34	2.5	0.627	0.83	8.0
<i>c</i>	-28	5.0	0.791	0.67	4.8
<i>d</i>	-20	8.0	0.925	0.52	2.9
<i>e</i>	-10	9.3	0.972	0.35	2.0
<i>f</i>	0	9.6	0.983	0.25	1.43
<i>g</i>	+20	9.8	0.989	0.18	0.80
<i>h</i>	+40	10.0	0.996	0.125	0.44

Curves *a*, *b*, *c*, *e* are demonstrated in Fig. 6;  $m_{\infty}$  was calculated by means of the equation (6).

with practical parameters  $m_{\infty}$ ,  $\tau_m$ ,  $h_{\infty}$  and  $\tau_h$  defined by

$$m_{\infty} = \alpha_m / (\alpha_m + \beta_m), \quad (6)$$

$$\tau_m = 1 / (\alpha_m + \beta_m), \quad (7)$$

$$h_{\infty} = \alpha_h / (\alpha_h + \beta_h), \quad (8)$$

$$\tau_h = 1 / (\alpha_h + \beta_h), \quad (9)$$

where  $\alpha$ 's and  $\beta$ 's are transfer rate constants.

Solving the equations 3—9 the following simplified formula (Hodgkin and Huxley 1952; Adrian et al. 1970) was obtained, and fitted to the experimental values of  $G_{Na}$  by computer, i.e.

$$G_{Na} = G'_{Na} [1 - \exp(-t/\tau_m)^3 \exp(-t/\tau_h)], \quad (10)$$

where  $t$  is time and  $G'_{Na}$  is the sodium conductance in the absence of inactivation.

The values of  $G'_{Na}$ ,  $m_{\infty}$ ,  $\tau_m$  and  $\tau_h$  obtained by the fitting procedure for different displacements of membrane potential  $V$  are given for the demonstrated fibre in Table 1.

The maximum sodium conductance,  $\bar{G}_{Na}$ , extrapolated from the  $G'_{Na} - V$  relation was  $10 \pm 7$  mS/cm<sup>2</sup> ( $\pm$  SEM). The relation between the membrane potential and  $m_{\infty}$  obtained from different denervated tonic muscle fibres is demonstrated in Fig. 7A. The maximum steepness of the  $m_{\infty} - V$  curve is 15 mV/e-fold change,

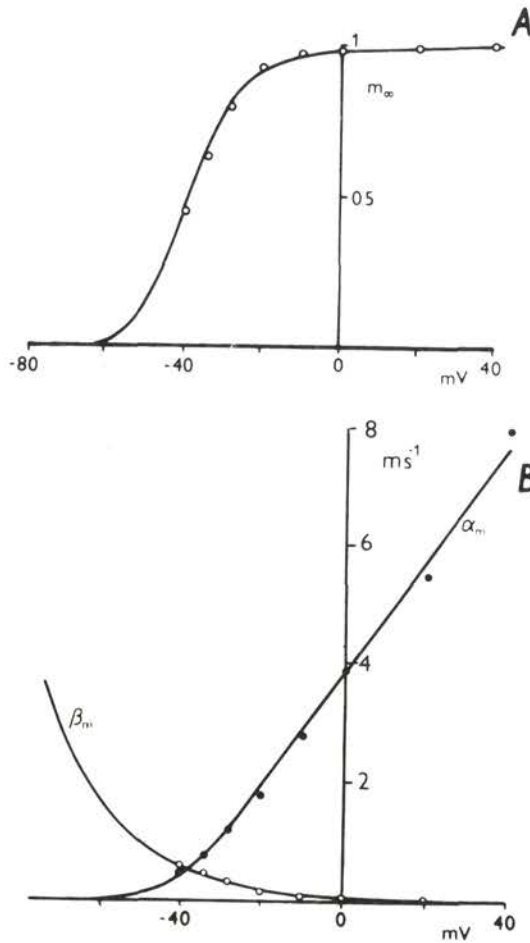


**Fig. 7.** Above: relation between membrane potential and  $m_\infty$ . The continuous curve was drawn according to equation (6). The experimental points are proportional to the third root of the sodium conductance ( $G_{\text{Na}}$ ). Below: relations between membrane potential and rate constants ( $\alpha_m$ ,  $\bullet$ ;  $\beta_m$ ,  $\circ$ ). The smooth curves are best fit lines through rate constants  $\alpha_m$  and  $\beta_m$  according to equations (11) and (12) respectively.

and the half value of  $m_\infty$  is at the membrane potential of  $-40$  mV.

The rate constants obtained from the analysis of the  $G_{\text{Na}} - V$  relations are demonstrated in Fig. 7B. The continuous curves represent the best fit solutions of the empirical equations (11) and (12) respectively:

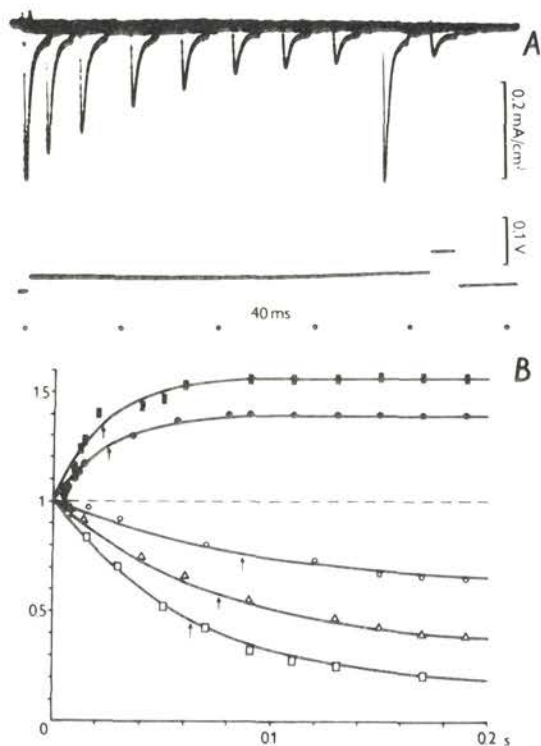


**Fig. 8.** Time course of sodium inactivation and its determination by two pulse method. A: Records of inward currents to a constant test pulse, from the holding potential  $V_H = -80$  mV to  $-10$  mV, preceded by a conditioning depolarization (to  $-30$  mV). The pulses are shown on the lower beam for the last current trace. B. Graphical presentation of the inactivation measurements. *Abcissa*: duration of the conditioning step. *Ordinate*: symbols, sodium peak currents relative to normal sodium peak currents; smooth curves were drawn according equation (13). The time constant  $\tau_i$ , is shown by arrows. The time course of inactivation corresponding to records in A is shown by triangles.

$$\alpha_m = \frac{\bar{\alpha}_m (V - \bar{V}_m)}{1 - \exp - [(V - \bar{V}_m) / V_{\alpha, m}]}, \quad (11)$$

$$\beta = \bar{\beta}_m \exp - \frac{(V - \bar{V}_m)}{V_{\beta, m}}, \quad (12)$$

with the following parameters:  $\bar{\alpha}_m = 0.097$ ,  $\bar{\beta}_m = 0.55$ ,  $\bar{V}_m = 40$ ,  $V_{\alpha, m} = 5.5$ ,  $V_{\beta, m} = 18$ . The average parameters are shown in Table 2.

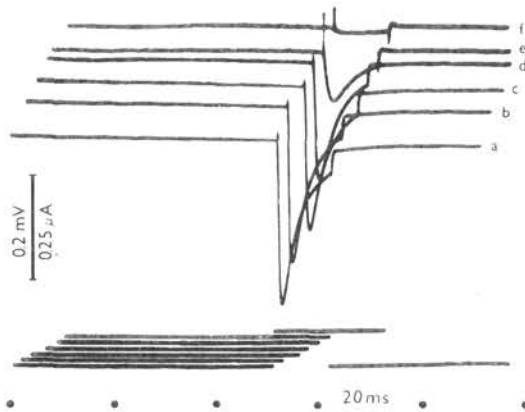


**Fig. 9.** Direct measurement of inactivation of sodium conductance by the two pulse method. The testing depolarizing pulse was constant (duration,  $t = 10$  ms; amplitude: 80 mV; displacement from  $V_h = -80$  mV). The conditioning pulse lasted 600 ms and its amplitude was varied in regular steps of 15 mV from *a* to *f* (with zero displacement in *a*).

#### *Inactivation of sodium conductance*

As follows from Fig. 6 and Table 1 the time constant of inactivation,  $\tau_h$ , decreases with the displacement of the membrane potential.  $\tau_h$  was determined from the conductance curves by means of equation (10), i.e. by fitting a single exponential to the decline of sodium current during depolarization (Method A). The assumption that  $h$  inactivates fully to zero in the steady state is less perfect, as can be seen in Fig. 6, which shows small deviations of the theoretical from the experimental time course of inactivation.

Fig. 8A shows the measurement of inactivation by the two-pulse method (Method B). The records show peak  $I_{Na}$  currents to a test pulse,  $V_t = -10$  mV from  $V_h = -80$  mV following a series of conditioning pulses of the same amplitude ( $V_c = -50$  mV) but of different duration. The peaks of the inward currents trace the time course of inactivation. Time course of inactivation at 5 different membrane potentials is demonstrated in Fig. 8B. Arrows denote  $\tau_h$ . It is evident that  $\tau_h$  decreases with depolarization. The continuous curves were calculated according to equation (13)

$$y = y_\infty - (y_\infty - 1) \exp(-t/\tau_h), \quad (13)$$

where  $y_\infty$  is the ordinate at  $t = \infty$  (the final steady level). The relation between  $y_\infty$  and the membrane potential is demonstrated in Fig. 10A (triangles). The other symbols represent values from direct measurements of  $h_\infty$  (Fig. 9). The continuous

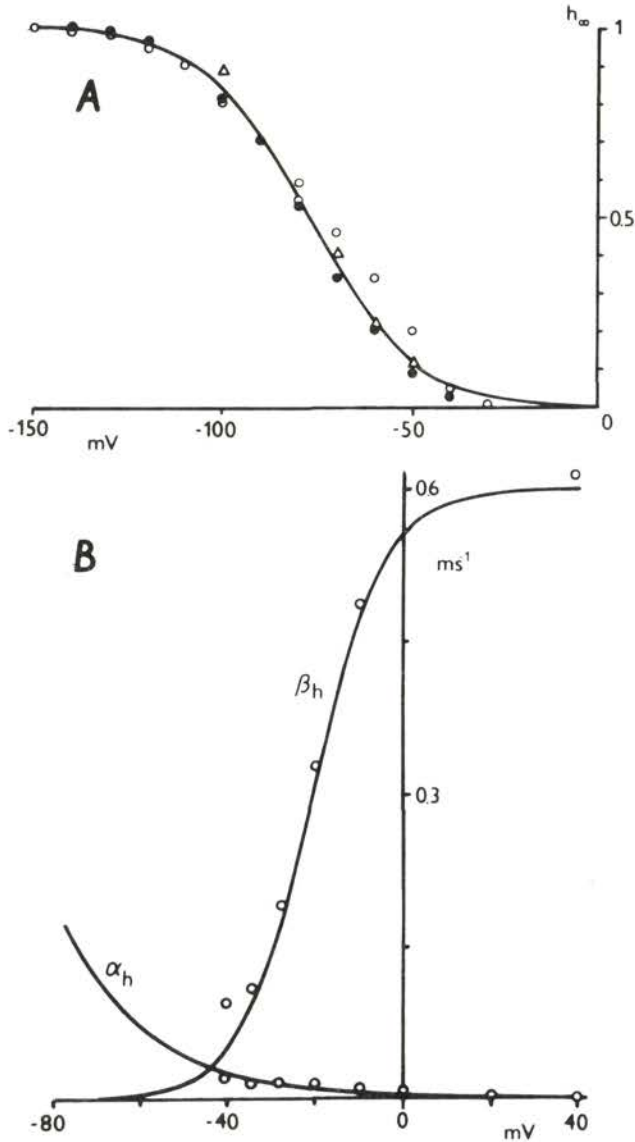


**Fig. 10.** Above: relation between membrane potential and  $h_{\infty}$ . The holding potential was  $-80$  mV. Symbols refer to different fibres. The data denoted by  $\Delta$  were obtained by the two pulse method (Fig. 8); all other by the method demonstrated in Fig. 9. The smooth curve was drawn according to equation (14). Below: relations between membrane potential and rate constants  $\alpha_h$  and  $\beta_h$  were drawn according to equations (17) and (18).

**Table 2.** Sodium channel parameters derived from voltage-clamp analysis

Parameter	<i>Loligo</i> axon (6.3°C)		Twitch fibres (5°C)		Tonic fibre (5°C)		
	1	2	3	4	5	6	7
$\bar{\alpha}_m$	ms <sup>-1</sup>	0.1	0.04	0.04	0.04	0.04	0.023
$\bar{\beta}_m$	ms <sup>-1</sup>	0.996	0.41	0.46	0.60	0.60	0.09
$\bar{V}_m$	mV	-37	-42	-42	-57	-57	-44
$V_{\alpha,m}$	mV	10	10	10	5	5	5
$V_{\beta,m}$	mV	18	18	18	13.7	13.7	18.7
$\alpha_h$	ms <sup>-1</sup>	0.01	0.003	0.00012	0.00012	0.00012	0.0019
$\beta_h$	ms <sup>-1</sup>	0.11	0.65	0.9	0.89	0.89	0.279
$\bar{V}_h$	mV	-32	-41	-25	-25	-25	-20
$V_{\alpha,h}$	mV	20	14.7	11	11	11	20
$V_{\beta,h}$	mV	10	7.6	13.6	13.6	13.6	11

(3) Hodgkin and Huxley (1952); *Loligo forbesi*

(4) Adrian, Chandler and Hodgkin (1970); *R. temporaria*

(5) Campbell and Hille (1976); *R. pipiens*

(6) Ildefonse and Roy (1972) measured at 20–23°C; *R. esculenta*

(7) this paper (denervated fibre), *R. temporaria*; measured at 16°C; scaled to 5°C assuming  $Q_{10}$  of 3.6 ( $n=4$ )

curve was fitted to the experimental points according to equation (14)

$$h_{\infty} = \left[ 1 + \exp \left( \frac{V - V_h}{V'_h} \right) \right]^{-1}, \quad (14)$$

where  $V_h = -77$  mV is the value of  $V$ , at which  $h_{\infty} = 0.5$ ;  $V'_h = -14$  mV is a constant, which characterizes the steepness of the curve.

The rate constants of inactivation (Fig. 10B) were determined by means of the  $h_{\infty} - V$  relation from the  $\tau_h$  values obtained by both the method A and B, according to the equations (15) and (16)

$$\tau_h = 1/(\alpha_h + \beta_h), \quad (15)$$

$$h_{\infty} = \alpha_h \tau_h \quad (16)$$

The full lines through the values of  $\alpha_h$  and  $\beta_h$  are theoretical lines according to the equations (17) and (18)

$$\alpha_h = \bar{\alpha}_h \exp - \frac{(V - \bar{V}_h)}{V_{\alpha,h}} \quad (17)$$

$$\beta_h = \bar{\beta}_h \left[ 1 + \exp - \frac{(V - \bar{V}_h)}{V_{\beta,h}} \right]^{-1} \quad (18)$$

with the following parameters:  $\bar{\alpha}_h = 0.01$  ms,  $\bar{V}_h = -20$  mV,  $V_{\alpha,h} = 20$ ,  $\bar{\beta}_h = 0.6$  ms and  $V_{\beta,h} = 8$ . Average values of these parameters are shown in Table 2.

## Discussion

This paper presents a kinetic analysis of the sodium currents which appear in slow (tonic) muscle fibres of the frog after denervation. The ability of slow muscle fibre membrane to generate spikes after denervation was discovered in early seventieth (Miledi et al. 1971), but the underlying ionic currents have not been analysed so far, most probably due to lack of suitable voltage clamp methods. We applied for this purpose the vaseline-gap technique developed by Hille and Campbell (1976) for cut muscle fibre segments. This method has several advantages over the three-microelectrodes voltage clamp method of Adrian et al. (1970), which was applied recently to analysis of ionic currents in normal tonic fibres by Gilly and Hui (1980). First, it offers a good voltage control for early events (sodium inward currents) after the voltage-clamp step; second, the inward ionic currents can be analysed under these conditions (cut muscle fibre segments) in potassium free environment, and third, the contractile apparatus can be kept easily relaxed by means of 'internal' relaxing solutions containing EGTA and ATP. A disadvantage is that the artificial internal solutions might change the membrane properties in an unanticipated way.

The main qualitative differences between the sodium currents in normal twitch muscle fibres of the frog and in slow muscle fibres after denervation are as follows. (1) The rate of rise and decay of inward sodium currents in slow muscle fibres is approximately one order of magnitude slower than in twitch fibres; (2) the maximum inward current in slow fibres is also about ten times lower than in twitch muscle fibres.

The sodium currents in slow muscle fibres are, however, similar to those in twitch muscle fibres and the mathematical Hodgkin-Huxley model which has been developed for sodium channel gating in twitch muscle fibres (Adrian et al. 1970) can be used to describe the kinetics of sodium currents in the denervated slow muscle membrane as well. The parameters of kinetic model of sodium channel conductance in twitch and slow muscle fibre membrane are compared in Table 2.

The rate constants parameters  $\bar{\alpha}_m$ ,  $\bar{\beta}_m$  and  $\bar{\beta}_h$  are fairly similar in three phasic muscle membranes; they are, however, lower by 1/2, 4/5 and 2/3, respectively in

slow fibres. Twitch fibres themselves differ considerably in their  $\bar{\alpha}_h$  values. The  $\bar{\alpha}_h$  in slow fibres is close to the highest value of  $\bar{\alpha}_h$  observed in twitch muscle membranes. The other kinetic parameters of sodium channels are fairly similar in both twitch and slow muscle membranes as well as in nerve membranes.

Denervation is known to change also the membrane properties of the twitch muscle fibres (Gutmann 1962, 1976; Thesleff 1974). In mammalian muscle membranes a new sodium channel is reported to appear after denervation (Pappone 1980) which might be responsible for the TTX resistant action potentials of the denervated mammalian muscle (Harris and Thesleff 1971). These relatively tetrodotoxin insensitive channels respond less rapidly to potential changes and can contribute up to 1/3 of the total  $G_{Na}$ . The new sodium channels which appear after denervation in tonic fibres of the frog also show a slower kinetics in comparison with Na channels in normal phasic fibres; they are, however, toxin sensitive as demonstrated in Fig. 5. It should be noted, however, that TTX changes the kinetics of sodium currents, as clearly evident, when the 'on' and the 'off' effects of TTX on sodium currents in Fig. 5 are compared. The nature of this effect remains unknown.

The selectivity of the sodium channels appearing after denervation in tonic (slow) fibre is very close to the selectivity of Na channels in normal twitch fibres from the frog (Zacharová et al. 1983). It therefore seems reasonable to assume, at least as a working hypothesis, that the new sodium channels represent the same channel moiety both in twitch and slow muscle fibre membranes. The only real difference concerns the rate of gating, which could be explained by the differences in composition of the membrane matrix itself.

## References

- Adrian R. H., Chandler W. K., Hodgkin A. L. (1970): Voltage clamp experiments in striated muscle fibres. *J. Physiol. (London)* **208**, 607—644
- Costantin L. L. (1975): Contractile activation in skeletal muscle. *Progr. Biophys. Molec. Biol.* **29**, 197—224
- Gilly W. F., Hui C. S. (1980): Membrane electrical properties in frog slow muscle fibres. *J. Physiol. (London)* **301**, 157—173
- Gulišek D., Henček M. (1978): Operational amplifier with adjustable frequency response. *Physiol. Bohemoslov.* **27**, 179—184
- Gutmann E. (1962): *The Denervated Muscle*. Publishing House of the Czechoslovak Acad. Sci., Prague
- Gutmann E. (1976): Neurotrophic relations. *Annu. Rev. Physiol.* **38**, 177—216
- Harris J. B., Thesleff S. (1971): Studies on tetrodotoxin resistant action potentials in denervated skeletal muscle. *Acta Physiol. Scand.* **84**, 382—388
- Henček M., Zachar J. (1977): Calcium currents and conductances in the muscle membrane of the crayfish. *J. Physiol. (London)* **268**, 51—71
- Henček M., Zacharová D., Zachar J. (1983): Properties of sodium channels in twitch muscle fibre membrane of the frog after denervation. *Gen. Physiol. Biophys.* **2**, (in press)

- Hess A. (1970): Vertebrate slow muscle fibres. *Physiol. Rev.* **50**, 40—62
- Hille B., Campbell D. T. (1976): An improved vaseline gap voltage clamp for skeletal muscle fibers. *J. Gen. Physiol.* **67**, 265—293
- Hodgkin A. L., Huxley A. F. (1952): A quantitative description of membrane current and its application to conduction and excitation in nerve. *J. Physiol. (London)* **117**, 500—544
- Ildefonse M., Roy G. (1972): Kinetic properties of the sodium current in striated muscle fibres on the basis of the Hodgkin-Huxley theory. *J. Physiol. (London)* **227**, 419—431
- Kuffler S. W., Vaughan Williams E. M. (1953): Properties of the slow skeletal muscle fibres of the frog. *J. Physiol. (London)* **121**, 318—340
- Lännergren J. (1973): Structure and function of twitch and slow fibres in amphibian skeletal muscle. In: *Basic Mechanisms of Ocular Mobility and Their Clinical Implications* (Eds. G. Lennerstrand, P. Bach-Y-Rita). pp. 63—84, Pergamon Press, Oxford, New York
- Lapshina I. B., Nasledov G. A. (1978): Changes of contractile properties in tonic muscle fibres after denervation. *Fiziol. Zh. SSSR (Leningrad)* **64**, 1129—1133 (in Russian)
- Miledi R., Stefani E., Steinbach A. B. (1971): Induction of the action potential mechanism in slow muscle fibres of the frog. *J. Physiol. (London)* **217**, 737—754
- Nasledov G. A. (1981): Tonic Muscle System of Vertebrates. Nauka, Leningrad (in Russian)
- Nasledov G. A., Thesleff S. (1974): Denervation changes in frog skeletal muscle. *Acta Physiol. Scand.* **90**, 370—380
- Nasledov G. A., Zachar J., Zacharová D. (1966): The ionic requirements for the development of contracture in isolated slow muscle fibres of the frog. *Physiol. Bohemoslov.* **15**, 293—306
- Nonner W. (1969): A new voltage clamp method for Ranvier nodes. *Pflügers Arch.* **309**, 176—192
- Pappone P. A. (1980): Voltage-clamp experiments in normal and denervated mammalian skeletal muscle fibres. *J. Physiol. (London)* **306**, 377—410
- Reich E., Cerami A., Ward D. C. (1967): Actinomycin. In: *Antibiotics. I. Mechanism of Action* (Eds. D. Gottlieb and P. D. Shaw), pp. 714—725, Springer-Verlag, New York
- Schalow G., Schmidt H. (1975): Effect of temperature and length of nerve stump on development of action potentials in denervated frog slow muscle fibres. *Pflügers Arch.* **335**, (Suppl.) R57
- Schmidt H., Stefani E. (1977): Reinnervation of twitch and slow fibres of the frog after crushing the motor nerves. *J. Physiol. (London)* **258**, 99—123
- Schmidt H., Stefani E. (1977): Action potentials in slow muscle fibres of the frog during regeneration of motor nerve. *J. Physiol. (London)* **270**, 507—517
- Schmidt H., Tong E. Y. (1973): Inhibition by actinomycin D of the denervation induced action potentials in frog slow muscle fibres. *Proc. Roy. Soc. B (London)* **184**, 91—95
- Thesleff S. (1974): Physiological effects of denervation of muscle. *Ann. New York Acad. Sci.* **228**, 89—104
- Zachar J. (1971): *Electrogenesis and Contractility in Skeletal Muscle Cells*. University Park Press, Baltimore and London
- Zacharová D., Zachar J., Henček M., Nasledov G. A. (1983): Selectivity of sodium channels in denervated tonic muscle fibre membrane of the frog. *Gen. Physiol. Biophys.* **2**, (in press)
- Zhukov E. K. (1969): *Studies on Nerve-Muscle Physiology*. Nauka, Leningrad (in Russian)